Application of Photographic Pyrometry to Ablation Models

Reginald J. Exton*
NASA Langley Research Center, Hampton, Va.

Surface temperature measurements on ablation models are described that demonstrate the application of photographic pyrometry to arcjet, arc tunnel, and rocket exhaust facilities. Sharp temperature discontinuities and hot spots are shown to be a predominant characteristic of the ablative surfaces tested, increasing the importance of spatial temperature measurements. The photographic pyrometry technique is, therefore, extremely valuable for determining point temperatures on the rough temperature contours, whether produced naturally as a result of the ablation process or by immersion sensors of vastly different thermal properties than the ablation material. The restrictions placed on the optical measurements by extraneous radiation are discussed and, in general, are found to be minor. An accuracy of 2–3% is estimated for these tests in the temperature range 1250–3800°K encompassing a possible inaccuracy of approximately ±14% in the mean emittance estimate of 0.88 for the ablators.

Introduction

Surface temperature measurements on ablative materials are extremely difficult in ground tests as well as in actual flight. Advanced thermocouple techniques are severely limited because of the lack of suitable high-temperature insulators, the oxidation environment, and the electrical properties of the gas cap. In addition, the temperature of the thermocouple junction is never that of the surrounding material because of the disparity in the thermal properties of the thermocouple and ablation materials. At re-entry heating rates, this temperature difference can become extremely large.[1] Substantial efforts have been and are being expended to develop improved immersion sensors and analysis techniques for flight use.[2–4]

For ground tests in a simulated re-entry environment, remote optical sensing techniques of the surface temperature are usually more reliable and accurate than immersion sensors. Many optical pyrometers have been developed utilizing brightness, ratio, and total radiation techniques that are useful for aerodynamic testing[5–7] and standard operation and calibration procedures have been described for optical pyrometry.[8] These instruments are in general restricted to single point measurements, however, and the accuracy is degraded by small model movements or facility vibrations. Many of these limitations are overcome by the photographic pyrometer technique[9,10] which effectively obtains a temperature measurement of all points within its field of view.

The purpose of this paper is to demonstrate the capability and versatility of this high surface temperature recording technique. The tests to be discussed were conducted in arcjet, arc tunnel, and a rocket exhaust facility.

Photographic Pyrometer Technique

The theory and operation of the variable exposure photographic pyrometer have been described in detail previously.[9,10] The pyrometer photographs the radiating surface at many different exposure levels through the use of a rotating variable density filter. Several of the photographs obtained in this manner are located on the linear portion of the film characteristic curve, where the relative surface brightness of selected points on the model can be measured. Calibration of the photographic pyrometer is obtained by photographing a source of known temperature and emittance on the same film as the unknown.

Received October 7, 1968; revision received June 9, 1969.
* Physicist, Instrument Research Division.

The photographic pyrometer used in these tests is shown in Fig. 1. This model is an improved version of those discussed in Ref. 10 in that it can be aligned without disturbing the film and is more compact and simple to operate than previous models. The rotating filter in this system is a neutral density circular wedge with a density range of 0 to 5.0. A fixed position balancing wedge is used in conjunction with the rotating wedge in order to render a uniformly attenuated image. The filter wheel is rotated at 1 cycle/sec and the camera is started by a cam operated switch coupled to the filter wheel. The camera then exposes one sequence (18 frames) at the rate of 20 frames/sec. A sequence is recorded each second for the duration of the test. A tungsten ribbon filament lamp is photographed before and/or after each test for use as a standard. The lamp temperature is set either by a calibrated brightness pyrometer or by a calibrated lamp–ammeter combination. Laboratory tests using a tungsten ribbon filament lamp as a standard show that the pyrometer exhibits an error of approximately 1% for temperatures in the range 1250–2750°K.

The film densities are read on a specially built contour densitometer shown in Fig. 2. In this instrument, light transmitted through the film is viewed on a large screen. An internally mounted beam splitter diverts part of the light intensity to form another image internally. At this second image, the photoelectric head of a densitometer equipped with a circular aperture is placed corresponding to a circular reticle on the viewing screen. An x-y stage allows movement of the film so that the density of selected points of interest may be recorded. With a film to screen magnification of 10×, the instrument is capable of reading the density of 0.13-mm-diam spots in the film plane. The film transport mechanism, mounted on the x-y stage, is capable of frame by frame, sequence by sequence, and cine motion for ease in readout selection.

High-Temperature Calibration

The application of photographic pyrometry to surface temperatures in the range 2750–3800°K requires an extrapolation in temperature far beyond that provided by a tungsten lamp. A tungsten ribbon filament lamp (GE 75A/T24) set at 2750°K is usually used as a standard since it is easily transportable and easy to operate in the restricted space available in most testing facilities. A check of the radiance (temperature) extrapolation is afforded in the laboratory with a low-current carbon arc. The arc is manufactured by the Mole-Richardson Company and is designated as the Pyrometric Molarc Lamp. The electrodes are continuously fed, the feed rate of each electrode being controlled separately. With a 6.4-mm-diam grade SPK graphite anode and a 3.2-mm-diam grade AGKS cathode, the spectral radiance of the anode center approximates a 3792°K blackbody over most of the wavelength range of the pyrometer.[11] Below 4200Å, appreciable divergence from the blackbody curve occurs due to the addition of line and band radiation in the arc column. The arc is supplied with a set of five filters that simulate lower temperatures for calibration of brightness pyrometers operating at 6500Å. These filtered temperatures are not directly applicable to the photographic pyrometer calibration since the filters are not neutral, decreasing in transmission from the appropriate pyrometric value at 6500Å to zero at approximately 4000Å.

Because of the filter problem, only direct views of the anode were used in the calibration. This affords a check on the extrapolation even though it restricts the high-temperature calibration to only one temperature. A tungsten ribbon filament lamp was used as a standard and the mean emittance was taken to be 0.44 for the wavelength range 3800–6700Å corresponding to the Tri-X pan film. The mean emittance for the SPK graphite was taken to be 0.99 for the same range.[12] The direct views of the anode yielded temperatures which were as much as $2\frac{1}{2}\%$ high. This is due to the large band radiation in the arc column below 4200Å. A wratten No. 3 filter was employed to restrict the pyrometer to wavelengths above 4200Å and a modified master cuve was computed for use with the filter. The direct views were then determined to be within 1% of the NBS value of 3792°K.

Facility Tests

The results of temperature measurements on ablation models in three different types of re-entry simulation facilities will be discussed in this section. These tests were performed in arcjet, arc tunnel, and rocket exhaust facilities. Each model environment will be analyzed to show the restrictions placed on an optical temperature measurement in that particular facility.

It will be seen that sharp temperature discontinuities and hot spots are a predominant characteristic of the ablation surfaces. The photographic pyrometer technique becomes even more attractive for measurements on these surfaces since single point devices would have vastly different results for a small change in positioning or would record an average temperature, depending on the spatial resolution.

Additional information concerning the model's interaction with its environment is often obtained as a result of acquiring pictures at different levels of exposure. Gas cap, spalling, and separated flow phenomena can often be studied through the use of these pictures.

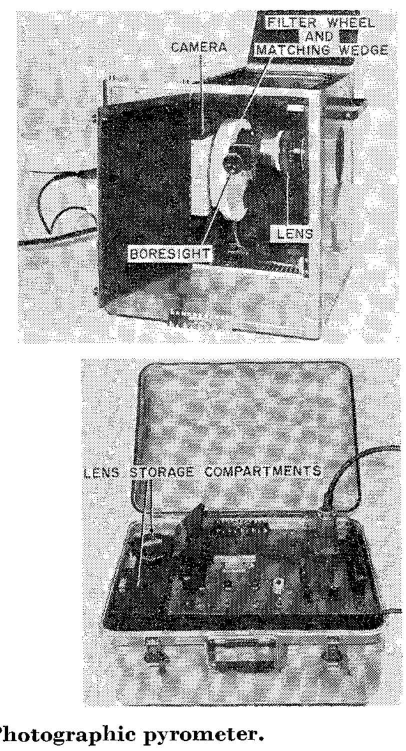

a) Optical components

b) Control package

Fig. 1 Photographic pyrometer.

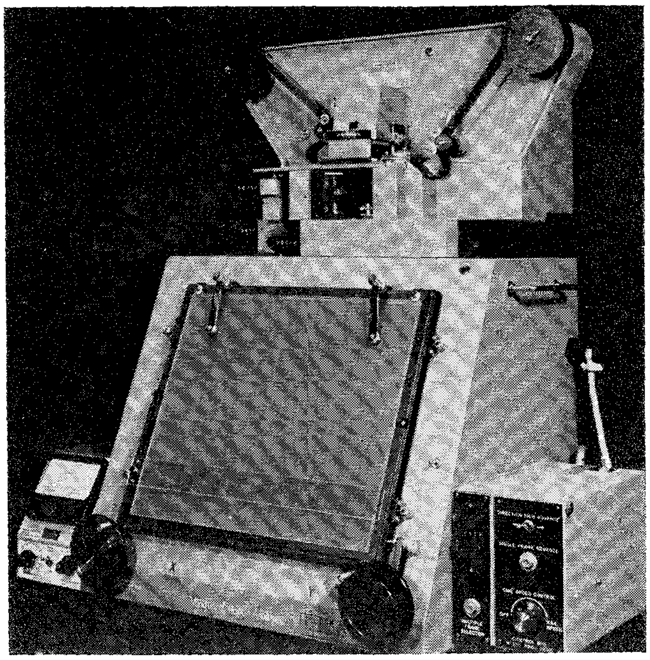

Fig. 2 Contour densitometer.

Arcjet Tests

These tests were performed in the Langley 2500 kw arcjet exhausting into the atmosphere through a 3.8-cm-diam nozzle. A maximum operating stagnation pressure of 244 kN/m^2 and stagnation temperature of 3800°K behind the model bow shock are possible with this nozzle. In this facility, the flow direction is vertical and the test specimen is swung into position on a water cooled support. The pyrometer is situated slightly below the model elevation affording a view of the front surface of the model from approximately 20° below the horizontal. The specimen was a 1.25-cm-diam flat face cylindrical model of phenolic carbon mounted on a tapered bakelite base. A heating rate of 9.1 Mw/m^2 was imposed on the model at slightly greater than sonic speed.

Figure 3 shows the initial frames of four sequences taken 1 sec apart. The first sequence shows the radiance of the freestream of the open arc, where the first few shock diamonds can be seen. This radiation is composed mainly of copper lines, sodium lines, and copper oxide bands as determined by a separate spectral survey. Although the gas temperature in the free stream is relatively high (of the order of 3400°K), the total intensity from all of these spectral lines is small with respect to the continuum radiation from heated bodies. Thus, the freestream intensity is recorded only in the first frames where the filter transmission is high.

The second sequence shows the model entering the stream and coming to a stable position. Approximately 8 frames (0.4 sec) is required from the time the model is first seen to the time it becomes stabilized.

The third sequence shows the well-stabilized model situated slightly off-axis in the stream. This is evidenced by the asymmetry of the gas cap and the streaming ablation products as seen in the first few frames along with the freestream. In the fourth frame, the intensity from the model is much higher

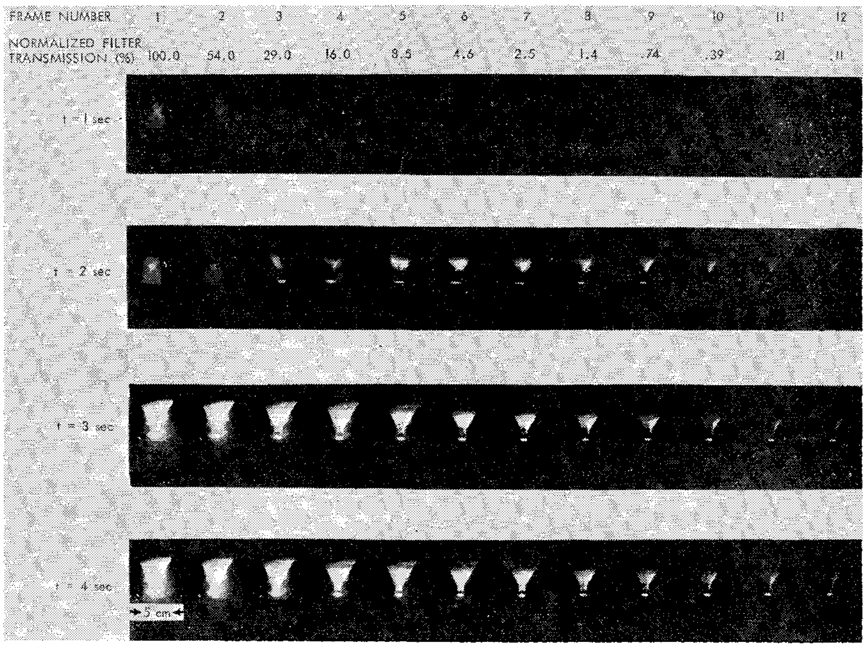

Fig. 3 Partial sequences of a phenolic carbon model in a 2500 kw a.c. arc-jet.

than that from the gas cap. Their relative intensities cannot be determined in this frame solely, however, since the model intensity is well on the over-exposed portion of the film characteristic curve. Approximately five frames later (filter transmission down by factor of about 20), the side wall temperatures would be recorded. At that point, the gas cap intensity is imperceptible. Still further down in transmission (higher intensity) the stagnation-point temperature would be recorded. The fourth sequence is similar to the preceding one with the exception that the model surface temperature has increased slightly. These considerations demonstrate that the gas cap and freestream radiances will not affect the steady-state surface temperature determinations. The steady-state stagnation temperatures recorded on the flat face of the phenolic carbon cylinder in this sequence are of the order of 2840°K. Side temperatures on the cylinder reach 2480°K. Temperatures recorded on the bakelite cone range from 2230°K to 2600°K. The estimated accuracy of these temperatures is 2–3% and is primarily controlled by emissivity estimates and problems associated with halation in the film and the resolution of the readout densitometer. Lower temperatures are present as evidenced by dark regions in the photograph. These temperatures are either below the sensitivity limits of the instrument as adjusted or are of such a nature that they are overshadowed by halation from adjacent hot regions in the earlier frames in which their temperatures would be recorded.

The possibility of extraneous results due to reflected light intensity can be a problem when recording low temperatures (early frames of a sequence). The effect of reflected radiance at the stagnation point emanating from the arc can be seen by comparing the intensities seen through a given frame as a function of time. Assuming the arc radiance to be constant in time, the reflected radiance should also be constant within the limits of a change of surface reflectance. Comparing the intensities in frame five for the last three sequences in Fig. 3 shows a sizeable increase in intensity (factor of approximately 20). This represents an increase in intensity over and above any reasonable change in surface reflectance and is taken to be due to an increase in the temperature. In addition, it is assumed that the reflectance of an ablator would decrease since the surface becomes very rough during ablation (emissivity approaches one) and this would further minimize the reflectance problem. Note also the increase in the radiance (temperature) at the side wall of the cylindrical carbon model where reflected arc radiance would be negligible.

For this facility, the reflected light problem seemed large considering the spectral line character of the arc. For this reason, photographic pyrometer pictures were taken of the water cooled arc electrodes. This was performed by viewing the electrodes by way of a front surfaced mirror suspended above the arc facility. The pictures show basically cold electrodes with hot spots appearing abruptly at random locations. These spots are believed to be molten copper which has a boiling point of 2610°K. This belief is substantiated by the recovery of splattered bits of copper from the surface of the suspended mirror. These hot spots will probably contribute more to the radiance reflected by the model than will the arc itself and consideration of radiance change with time, as mentioned previously, should be employed to establish the valid temperature limits.

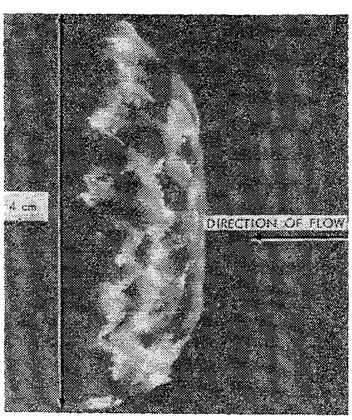

Fig. 4 Phenolic nylon model in a 2500 kw a.c. arc heated tunnel.

Arc Tunnel Tests

These tests were conducted in a 2500 kw a.c. arc heated tunnel using a one-half air, and one-half nitrogen mixture exhausting through a diffuser and heat exchanger into a vacuum tank. A heating rate of 4.3 Mw/m^2 was obtained at Mach 2. The tests were conducted on a flat face, cylindrical model 3.8 cm in diameter, constructed of low-density phenolic nylon and mounted on a retractable sting. The flow direction is horizontal in this facility and the pyrometer views the model from the side through a thick glass window in the test section. Calibration of the pyrometer is performed by placing a standard lamp within the test section before and after the test run and photographing it through the same window as for the test model. In this manner, changes in

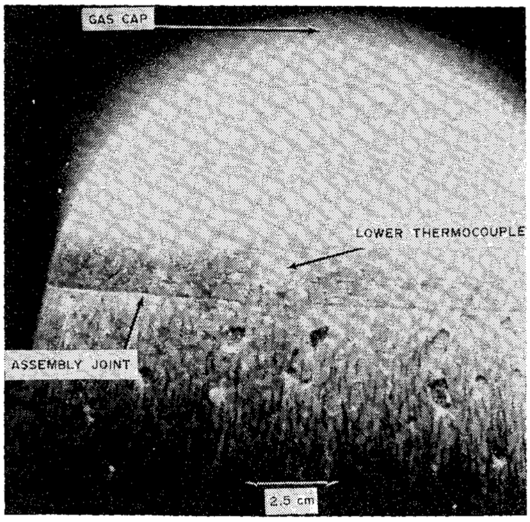

Fig. 5 Rocket exhaust model—illustrating the gas cap.

the window transmission due to contamination deposits during the run can be taken into account if necessary.

These tests demonstrate an extreme example of temperature discontinuity and the ability of the photographic pyrometer to record it. The flat face model is gradually eroded with time, resulting in the rounded shape shown in Fig. 4. The surface gives the appearance of being in a molten, flowing state, although the pattern is a relatively stable one. The main point to be emphasized with this surface is the extreme temperature gradients, the hot regions (2420–2560°K) being approximately 1000° hotter than the adjacent cool ones. The ensuing difficulties in making thermodynamic calculations or in sensor development on such an ablator are obvious.

Rocket Exhaust Tests

These tests were conducted at Test Complex 4 of the General Electric Malta Test Station. The exhaust of a rocket engine is employed at this complex as a source of high-mass flow, high Mach number, and high-temperature gas for material investigations. The use of rocket exhausts allows the testing of larger models in a more uniform flow field and greater flexibility in the installation of prototype instrumentation.

A liquid oxygen–alcohol mixture was used as fuel for these tests. The engine was operated at Mach 2.86 with a heating rate of 25 Mw/m^2, a stagnation pressure of 1 MN/m^2, and a stagnation temperature of approximately 3300°K behind the model bow shock.

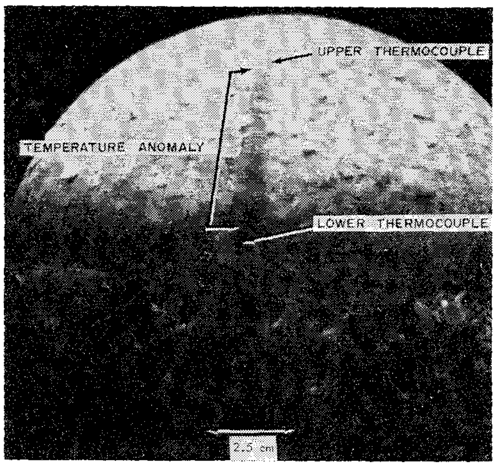

Fig. 6 Rocket exhaust model showing temperature anomaly originating at the upper thermocouple.

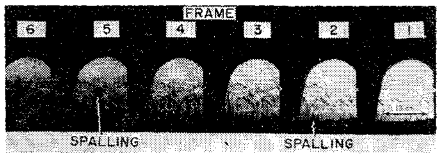

Fig. 7 Occurrence of spalls on the rocket exhaust model.

The cone shaped model, rounded at the apex, was constructed from phenolic carbon (37% phenolic resin by weight, 8% carbon filler by weight, and 55% of 6.4-mm-long carbon fibers) and mounted on water-cooled supports. It is 25.4 cm in diameter at its base and 35.5 cm high. Two ribbon type, tungsten vs tungsten/26% rhenium thermocouples were surface mounted in 1.25-cm-diam plugs near the tip of the model. A two-color ratio pyrometer was aligned to view an area adjacent to the rearmost thermocouple. The viewing area of the ratio pyrometer was a 2.5-cm-diam spot. The photographic pyrometer was situated about 2.4 m from the model, a distance at which the field of view encompassed the forward half of the model.

During the first few seconds of heating, the photographic pyrometer revealed only the model outline as it appears in the rocket exhaust. This establishes the fact that there will be no problem with respect to reflected radiation in the test environment. Several seconds later, the model has become self-luminous and Fig. 5 shows an over exposed picture of the model in which the gas cap is also visible. Shortly, thereafter, a properly exposed photograph (Fig. 6) reveals a vertical strip that is cooler than the surrounding areas. Since the strip originates at the thermocouple location, it can probably be attributed to either separated flow occurring at a protruding thermocouple or as material addition at that point. A qualitative spectral analysis of the burned material in the strip relative to the adjacent material with a 1.5m Wadsworth spectrograph did not exhibit any spectral lines of tungsten or rhenium. This is not a conclusive test, however, since the sensitivity limits of such an analysis were not known and it would be expected that the concentration would be very low.

The occurrence of spalling is illustrated in Fig. 7 showing six consecutive frames of a sequence. A large spall leaves the surface between the first and second frames of this series at the bottom of the pictures and another leaves between the fourth and fifth frames immediately below one of the thermocouple locations. The subsurface exposed following such an event generally has a temperature at least 600°K below the surface temperature of the spall itself.

The condition of the model toward the end of the test (total test time—10 sec) is shown in Fig. 8. The location of the two thermocouples is evidenced by dark spots indicating a heat sink due to the thermocouple itself. The dark spot temperatures as recorded by the photographic pyrometer are

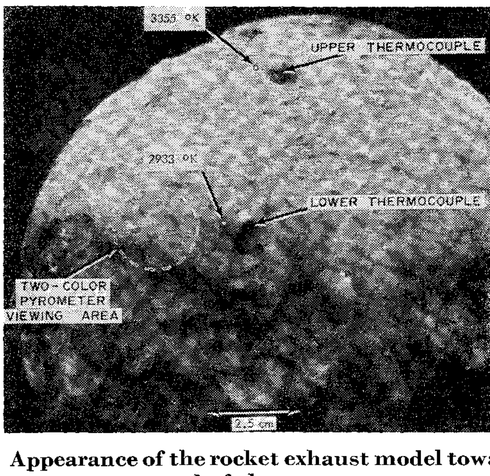

Fig. 8 Appearance of the rocket exhaust model toward the end of the test.

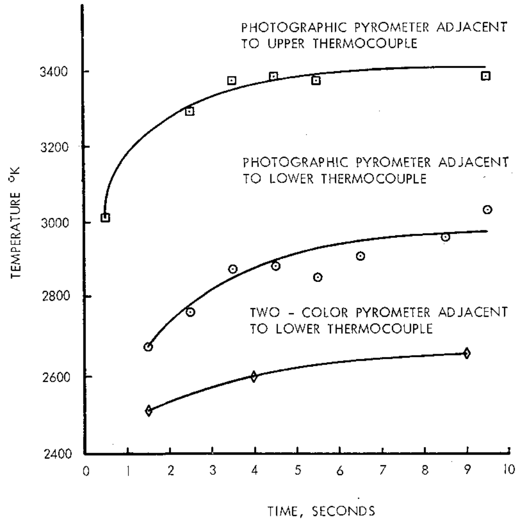

Fig. 9 Temperature measurements on a phenolic carbon model in a rocket exhaust.

generally several hundred to a thousand degrees cooler than the adjacent temperatures. The temperature as a function of time for the unperturbed regions adjacent to the thermocouples are shown in Fig. 9. The data from the two-color pyrometer adjacent to the lower thermocouple location is also plotted on this graph. The fact that the two-color pyrometer reads 8–10% below the photographic pyrometer may be justified since the photographic pyrometer data was recorded at a high-temperature point adjacent to the thermocouple, whereas the two-color pyrometer averages many high- and low-temperature spots due to its large viewing area. The accuracy of the photographic pyrometer measurements is estimated to be 2–3% encompassing a possible inaccuracy of approximately ±14% in the mean emittance estimate of 0.88.

The thermocouple data is not shown since it was extremely erratic, exhibiting numerous apparent changes in temperature as high as 700°K in $\frac{1}{10}$ of a second. This behavior is attributed to the repeated making and breaking of the contact in the thermocouple junction and the tendency of the exposed thermocouple to be influenced by the gas temperature. During the final seconds of the test, the upper thermocouple ranges from 3250 to 3690°K, whereas the lower thermocouple ranges from 2610–2890°K.

Concluding Remarks

A photographic pyrometer has been described which exhibits approximately 1% error in a laboratory calibration with a tungsten ribbon filament lamp operated in the temperature range 1250–2750°K. A high-temperature calibration using the anode of a low-current carbon arc at 3792°K exhibits the same accuracy when a wratten No. 3 filter is used to eliminate unwanted band radiation from the arc column.

Ablation model tests conducted in arcjet, arc tunnel, and rocket exhaust facilities were described that demonstrated the capability of the pyrometer to determine high surface temperatures in severe oxidation and vibrational environments. Sharp temperature discontinuities and hot spots were shown to be a predominant characteristic of the ablative surfaces tested, increasing the importance of spatial temperature measurements. The photographic pyrometer technique is, therefore, extremely valuable for determining point temperatures on the rough temperature contours, whether produced naturally as a result of the ablation process or by immersion sensors of vastly different thermal properties than the ablation material. These tests indicate that photographic pyrometry can be used for surface temperature measurements on ablation models up to 3800°K with an estimated accuracy of 2–3%.

Additional information concerning the model's interaction with its environment can often be obtained as a result of acquiring pictures at various levels of exposure. Spalling and separated flow phenomena were demonstrated through the use of such pictures. The temperature measurements in these facilities were shown to be unaffected by the radiance from the free stream and gas cap regions, due to their small radiance relative to the surface under consideration. Reflectance of extraneous arc radiation by the model in the arc facilities, however, was shown to limit the temperature measurements to the higher values measured. Means for evaluating the useful temperature range under these conditions have been discussed.

Photographic pyrometry involves the photographing of the unknown surface and a calibration surface under controlled exposure conditions, controlled development of the film, and time consuming readout of the film densities of interest. It is one of the most difficult and tedious temperature measuring devices in existence, but is presently the best instrument for measurements on these surfaces and provides a reliable basis for evaluating immersion sensors. Studies are presently being conducted to extend the technique to lower temperatures through the use of high-speed infrared film and longer exposures.

References

[1] Nydick, S. E., "Thermocouple Errors in Ablation Materials," preprint 16.12-3-66, Oct. 24–27, 1966, Instrument Society of America.

[2] Johnson, W. P., "Ultra-High Temperature Thermocouple for Aerospace Application," *Proceedings of 12th National ISA Aerospace Instrumentation Symposium*, May 2–4, 1966, Philadelphia, Pa.

[3] Dow, M., "Comparison of Measurements of Internal Temperatures in Ablation Material by Various Thermocouple Configurations," TN D-2165, Nov. 1964, NASA.

[4] Popov, V. N., "Distortion of Temperature Field in the Region of Location of a Thermocouple," *High Temperature*, translation Vol. 4, March-April 1966, pp. 255–260.

[5] Hanst, P. L., "Surface Temperature Measurements on Ablating Missile and Satellite Heat Shield Materials," *Temperature*, Vol. III, Pt. 2, 1962, p. 489.

[6] Moffitt, G., "Study of Temperature Measuring System for the 1000°C to 2500°C Range," Rept. ASD-TR-61-487, 1962, Aeronautical Systems Div., Wright-Patterson Air Force Base.

[7] Stevens, R. J. and Hornfeck, A. J., "An Industrial Radiation Pyrometer Using a Vacuum Bolometer," *Temperature*, Vol. III, Pt. 2, p. 371, 1962.

[8] Kostkowski, H. J. and Lee, R. D., "Theory and Methods of Optical Pyrometry," *Temperature*, Vol. III, Pt. 1, p. 449, 1962.

[9] Exton, R. J., "Theory and Operation of a Variable Exposure Photographic Pryometer Over the Temperature Range 1800° to 3600°F (1255° to 2255°K)," TN D-2660, March 1965, NASA.

[10] Exton, R. J., "A Variable Exposure Photographic Pryometer," *ISA Transactions*, Instrument Society of America, Vol. 4, Oct. 1965, pp. 365–373.

[11] Hattenburg, A. T., "Spectral Radiance of a Low Current Graphic Arc," *Applied Optics*, Vol. 6, Jan. 1967, p. 95.

[12] Null, M. R. and Losier, W. W., "Measurement of Reflectance and Emittance at High Temperatures with a Carbon Arc Image Furnace," *Measurement of Thermal Radiation Properties of Solids—Symposium NASA SP-31*, NASA, Sept. 1962.